

Hyperbolic Busemann Neural Networks

Ziheng Chen, Bernhard Schölkopf, Nicu Sebe



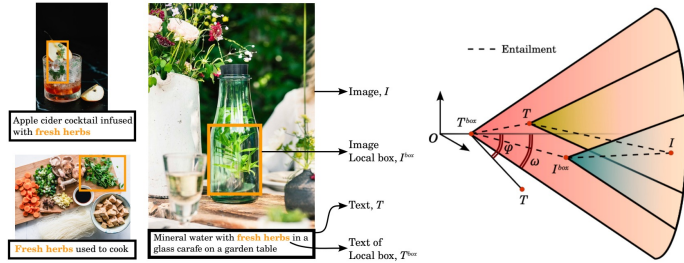
UNIVERSITÀ
DI TRENTO



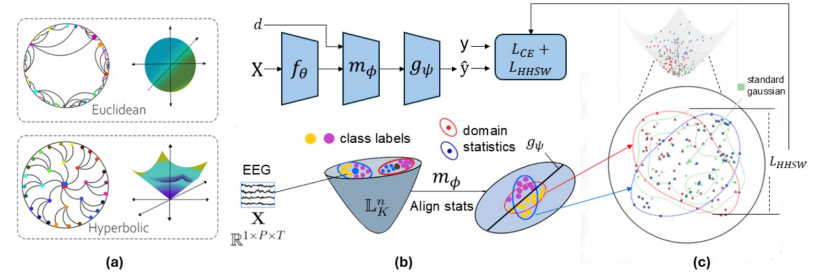
MAX PLANCK INSTITUTE
FOR INTELLIGENT SYSTEMS

Applications of Hyperbolic Spaces

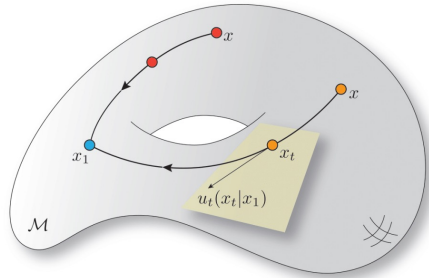
Vision-Language Models



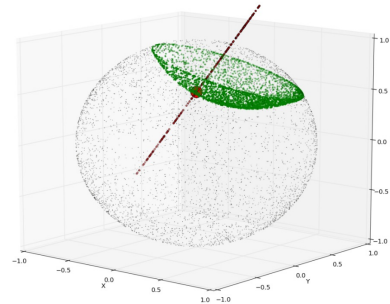
Brain-Computer Interfaces



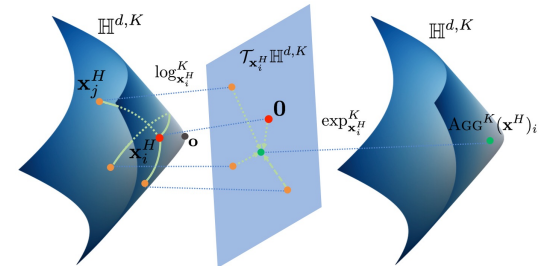
Generation



NLP



Graph





Definition

$$\forall x \in \mathcal{H}_K^n, \quad B^\gamma(x) = \lim_{t \rightarrow \infty} (d(x, \gamma(t)) - t).$$

$$H_\tau^v = \{x \in \mathcal{H}_K^n \mid B^v(x) = \tau\}$$

$$\forall x \in \mathbb{R}^n, \quad B^v(x) = -\langle x, v \rangle, \quad v \in \mathbb{S}^{n-1} = \{v \in \mathbb{R}^n \mid \|v\| = 1\}$$

Example

$$\mathbb{P}_K^n : B^v(x) = \frac{1}{\sqrt{-K}} \log \left(\frac{\|v - \sqrt{-K}x\|^2}{1 + K\|x\|^2} \right),$$

$$\mathbb{L}_K^n : B^v(x) = \frac{1}{\sqrt{-K}} \log \left(\sqrt{-K} (x_t - \langle x_s, v \rangle) \right).$$

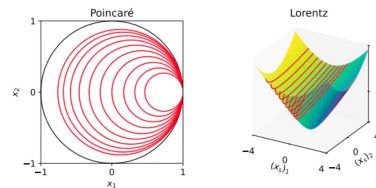


Figure 1. Illustration: red curves are different horospheres of B^v .

Table 1. Generalization: Euclidean vs. hyperbolic.

Generalization

Euclidean	Hyperbolic
Straight line	Geodesic
Parallel lines	Asymptotic geodesic rays
Inner product $\langle v, x \rangle$	Busemann function $-B^v(x)$
Hyperplane	Horosphere
Parallel hyperplanes with $v \in \mathbb{S}^{n-1}$	Horospheres with $v \in \mathbb{S}^{n-1} \cap T_e \mathcal{H}_K^n$

Euclidean MLR

$$\forall k, p(y = k | x) = \frac{\exp(\langle a_k, x \rangle + b_k)}{\sum_{j=1}^C \exp(\langle a_j, x \rangle + b_j)},$$

$$u_k(x) = \alpha_k \langle v_k, x \rangle + b_k.$$

$$v_k = \frac{a_k}{\|a_k\|} \in \mathbb{S}^{n-1} \quad \alpha_k = \|a_k\| > 0$$

$$d(x, H_{a_k, b_k}) = \frac{|\langle a_k, x \rangle + b_k|}{\|a_k\|}$$

$$H_{a_k, b_k} = \{x \in \mathbb{R}^n : \langle a_k, x \rangle + b_k = 0\}$$

$$u_k(x) = \text{sign}(\langle a_k, x \rangle + b_k) \|a_k\| d(x, H_{a_k, b_k}),$$

BMLR

$$\forall k, p(y = k | x) = \frac{\exp(u_k(x))}{\sum_{j=1}^C \exp(u_j(x))},$$

$$u_k(x) = -\alpha_k B^{v_k}(x) + b_k,$$

with $\alpha_k > 0$, $v_k \in \mathbb{S}^{n-1}$, and $b_k \in \mathbb{R}$ as parameters.

$$d(x, H_{v, \alpha, b}) = \frac{|-\alpha B^v(x) + b|}{\alpha}.$$

$$H_{v, \alpha, b} = \{x \in \mathcal{H}_K^n \mid -\alpha B^v(x) + b = 0\},$$

$$u_k(x) = \text{sign}_k \alpha_k d(x, H_{v_k, \alpha_k, b_k})$$

$$\text{sign}_k = \text{sign}(-\alpha_k B^{v_k}(x) + b_k)$$

BUSEMANN FULLY CONNECTED LAYER

Euclidean FC

$$y = Ax + b \in \mathbb{R}^m$$

$$y_k = \langle a_k, x \rangle + b_k$$

Interpretation



Hyperbolic interpretation

$$\bar{d}(y, H_{e_k,0}) = \langle a_k, x \rangle + b_k, \forall 1 \leq k \leq m,$$

$$\bar{d}(y, H_{e_k,0}) = \text{sign}(\langle e_k, y \rangle) d(y, H_{e_k,0})$$



Poincaré

$$y = \frac{\omega}{1 + \sqrt{1 - K \|\omega\|^2}}, \quad \omega = \left[\frac{\sinh(\sqrt{-K} u_k(x))}{\sqrt{-K}} \right]_{k=1}^m,$$

Lorentz

$$y = \begin{bmatrix} y_t \\ y_s \end{bmatrix} = \begin{bmatrix} \sqrt{\frac{1}{-K} + \|y_s\|^2} \\ \frac{1}{\sqrt{-K}} \sinh(\sqrt{-K} u(x)) \end{bmatrix}$$



Generalization

$$\bar{d}(y, H_{e_k,e}) = \phi(u_k(x)), \forall 1 \leq k \leq m.$$

$$\mathbb{L}_K^n \ni x \mapsto y = \begin{bmatrix} \sqrt{\frac{1}{-K} + \|y_s\|^2} \\ \frac{1}{\sqrt{-K}} \sinh(\sqrt{-K} u(x)) \end{bmatrix} \oplus_{\mathbb{L}} b \in \mathbb{L}_K^m,$$

COMPARISON



MLR

Real distance · Compact parameters · Batch-efficient

Method	Logit $u_k(x), \forall k \in \{1, \dots, C\}$	Space	Dist	#Params	Compact params	FLOPs	Batch efficiency
Euclidean MLR	$\langle a_k, x \rangle + b_k$, with $a_k \in \mathbb{R}^n, b_k \in \mathbb{R}$	\mathbb{R}^n	Real	$C(n+1)$	✓	$C(2n)$	✓
Poincaré MLR [23, Eq. (25)]	$\frac{\lambda_{pk}^K \ a_k\ }{\sqrt{-K}} \sinh^{-1} \left(\frac{2\sqrt{-K} \langle -p_k \oplus_M x, a_k \rangle}{(1+K \ -p_k \oplus_M x\ ^2) \ a_k\ } \right)$, with $p_k \in \mathbb{P}_K^n, a_k \in T_{p_k} \mathbb{P}_K^n$	\mathbb{P}_K^n	Real	$C(2n)$	✗	$C(19n+29)$	✗
Poincaré MLR [51, Eq. (6)]	$\alpha = \lambda_{pk}^K \sqrt{-K} \langle x, v_k \rangle \cosh(2\sqrt{-K} b_k)$, $\beta = (\lambda_{pk}^K - 1) \sinh(2\sqrt{-K} b_k)$, with $\alpha_k > 0, v_k \in \mathbb{S}^{n-1}, b_k \in \mathbb{R}$	\mathbb{P}_K^n	Real	$C(n+2)$	✓	$C(4n+52)$	✓
Pseudo-Busemann MLR [45, Cor. 4.3]	$-d(x, p_k) \frac{B^{v_k}(-p_k \oplus_M x)}{\ -p_k \oplus_M x\ }$, with $p_k \in \mathbb{P}_K^n, v_k \in \mathbb{S}^{n-1}$	\mathbb{P}_K^n	Pseudo	$C(2n)$	✗	$C(19n+34)$	✗
Lorentz MLR [3, Eq. (12)]	$\frac{1}{\sqrt{-K}} \text{sign}(\alpha) \beta \left \sinh^{-1} \left(\frac{\sqrt{-K} \alpha}{\beta} \right) \right $, $\alpha = \cosh(\sqrt{-K} b_k) \langle z_k, x_s \rangle - \sinh(\sqrt{-K} b_k)$, $\beta = \sqrt{\ \cosh(\sqrt{-K} b_k) z_k\ ^2 - (\sinh(\sqrt{-K} b_k) \ z_k\)^2}$, with $z_k \in \mathbb{R}^n, b_k \in \mathbb{R}$	\mathbb{L}_K^n	Real	$C(n+1)$	✓	$C(4n+52)$	✓
BMLR	$-\alpha_k B^{v_k}(x) + b_k$, with $\alpha_k > 0, v_k \in \mathbb{S}^{n-1}, b_k \in \mathbb{R}$	\mathbb{P}_K^n \mathbb{L}_K^n	Real	$C(n+2)$	✓	$\mathbb{P}_K^n: C(6n+12)$ $\mathbb{L}_K^n: C(2n+12)$	✓

FC

Busemann-based · Comparable complexity

Method	$\mathcal{F}: \mathcal{H}_K^n \ni x \mapsto y \in \mathcal{H}_K^m$	Space	Methodology	Parameters	#Params	FLOPs
Möbius [23, Eq. 27]	$\frac{1}{\sqrt{-K}} \tanh \left(\frac{\ Wx\ }{\ x\ } \tanh^{-1}(\sqrt{-K} \ x\) \right) \frac{Wx}{\ Wx\ }$	\mathbb{P}_K^n	Tangent	$W \in \mathbb{R}^{m \times n}$	mn	$2nm + 2n + 2m + 24$
Poincaré FC [51, Eq. (7)]	$y = \frac{\omega}{1 + \sqrt{1 - K \ \omega\ ^2}}$, $\omega_k = \frac{\sinh(\sqrt{-K} u_k(x))}{\sqrt{-K}}$, with $u_k(x)$ in Tab. 2	\mathbb{P}_K^n	Poincaré geometry	$\alpha_k > 0, v_k \in \mathbb{S}^{n-1}, b_k \in \mathbb{R}$, for $k = 1, \dots, m$	$m(n+2)$	$4nm + 71m + 4$
Lorentz FC [11, Eq. (3)]	$y = \left[\frac{\sqrt{\ \psi(Wx, v)\ ^2 - 1/K}}{\psi(Wx, v)} \right]$, $\psi(Wx, v) = \lambda \sigma(v^\top x + b) \frac{W\phi(x) + b}{\ W\phi(x) + b\ }$ with ϕ and σ as the activation and sigmoid	\mathbb{L}_K^n	Ambient Minkowski	$W \in \mathbb{R}^{m \times (n+1)}, v \in \mathbb{R}^{n+1}, b \in \mathbb{R}^m, b' \in \mathbb{R}, \lambda > 0$	$m(n+1) + m + (n+1) + 2$	$2nm + 8m + 2n + 10$
BFC	$y = \frac{\omega}{1 + \sqrt{1 - K \ \omega\ ^2}}$, $\omega = \frac{\sinh(\sqrt{-K} u(x))}{\sqrt{-K}}$, $y_s = \frac{1}{\sqrt{-K}} \sinh(\sqrt{-K} u(x))$, $y_t = \sqrt{\frac{1}{-K} + \ y_s\ ^2}$, with $u_k(x) = \phi(-\alpha_k B^{v_k}(x) + b_k)$	\mathbb{P}_K^n \mathbb{L}_K^n	Busemann	$\alpha_k > 0, v_k \in \mathbb{S}^{n-1}, b_k \in \mathbb{R}$, for $k = 1, \dots, m$	$m(n+2)$	$6nm + 29m + 4 + 2nm + 30m + 2$

Image

Image classification

Space	Method	CIFAR-10 (Num. classes: 10)			CIFAR-100 (Num. classes: 100)			Tiny-ImageNet (Num. classes: 200)			ImageNet-1k (Num. classes: 1000)		
		Acc	Fit Time	#Params	Acc	Fit Time	#Params	Acc	Fit Time	#Params	Acc	Fit Time	#Params
\mathbb{R}^n	MLR	95.14 ± 0.12	10.66	5.13K	77.72 ± 0.15	10.60	51.30K	65.19 ± 0.12	69.17	102.60K	71.87	2263.12	513K
\mathbb{P}_K^n	PMLR	95.04 ± 0.13	11.94	5.14K	77.19 ± 0.50	12.11	51.40K	64.93 ± 0.38	71.90	102.80K	71.77	2300.11	514K
	PBMLR-P	95.23 ± 0.08	21.92	10.24K	77.78 ± 0.15	76.84	102.40K	65.43 ± 0.27	336.58	204.80K	71.46	3907.12	1024K
	BMLR-P	95.32 ± 0.14	12.01	5.14K	78.10 ± 0.35	12.13	51.40K	66.16 ± 0.19	71.98	102.80K	73.36	2300.77	514K
\mathbb{L}_K^n	LMLR	94.98 ± 0.12	11.55	5.13K	78.03 ± 0.21	11.72	51.30K	65.63 ± 0.10	69.27	102.60K	72.46	2277.17	513K
	BMLR-L	95.25 ± 0.02	11.08	5.14K	78.07 ± 0.26	11.22	51.40K	65.99 ± 0.14	69.19	102.80K	73.24	2276.53	514K

Genome

Genome sequence learning

Benchmark	Task	Dataset	Num. classes	\mathbb{P}_K^n			\mathbb{L}_K^n	
				PMLR	PBMLR-P	BMLR	LMLR	BMLR-L
TEB	Retrotransposons	LTR Copia	2	75.34 ± 1.02	74.37 ± 1.48	76.73 ± 1.08	73.01 ± 1.07	75.86 ± 1.52
		LINEs	2	85.54 ± 0.61	85.92 ± 0.65	86.05 ± 1.08	83.14 ± 0.80	86.72 ± 0.58
		SINEs	2	95.30 ± 0.85	95.34 ± 1.58	95.99 ± 0.74	96.70 ± 0.87	96.29 ± 0.59
	DNA transposons	CMC-EnSpm	2	83.39 ± 0.56	83.62 ± 1.00	84.03 ± 0.71	81.78 ± 1.05	84.15 ± 1.00
		hAT-Ac	2	89.38 ± 0.90	89.86 ± 0.54	89.62 ± 0.74	88.94 ± 0.69	90.70 ± 0.51
	Pseudogenes	processed unprocessed	2	72.45 ± 1.49	71.99 ± 2.04	73.09 ± 1.66	73.71 ± 1.76	73.32 ± 1.65
2			75.37 ± 2.27	71.99 ± 1.47	75.71 ± 1.89	74.54 ± 1.98	76.15 ± 1.61	
Core Promoter Detection	tata notata all	2	80.95 ± 1.47	79.32 ± 2.44	80.29 ± 1.63	80.90 ± 1.15	81.76 ± 1.16	
		2	70.02 ± 0.52	70.60 ± 0.75	70.48 ± 0.35	71.26 ± 0.56	70.43 ± 0.39	
		2	67.64 ± 0.77	68.02 ± 0.63	68.50 ± 0.61	67.63 ± 0.56	68.36 ± 1.07	
GUE	Promoter Detection	tata	2	80.30 ± 1.59	80.27 ± 2.71	82.83 ± 1.69	83.27 ± 1.95	82.55 ± 1.54
		notata	2	92.63 ± 0.36	93.05 ± 0.32	92.75 ± 0.51	91.74 ± 0.57	92.60 ± 0.49
		all	2	90.53 ± 0.50	90.79 ± 0.77	90.20 ± 0.65	89.34 ± 0.40	89.82 ± 0.45
Covid Variant Classification	Covid	9	74.09 ± 0.25	70.84 ± 0.80	73.40 ± 0.30	64.07 ± 0.51	72.45 ± 0.21	
Species Classification	Virus	20	67.24 ± 2.10	59.17 ± 3.32	77.12 ± 1.23	71.34 ± 2.05	77.21 ± 1.04	
	Fungi	25	15.06 ± 1.32	18.75 ± 1.77	30.01 ± 0.76	15.07 ± 1.88	30.14 ± 2.48	

Graph

Node classification

Space	Method	Disease $\delta = 0$	Airport $\delta = 1$	PubMed $\delta = 3.5$	Cora $\delta = 11$
\mathbb{P}_K^n	HGCN	86.87 \pm 2.58	85.34 \pm 1.16	76.29 \pm 0.98	76.56 \pm 0.81
	HGCN-PMLR	88.98 \pm 1.96	84.78 \pm 1.48	76.02 \pm 1.09	77.47 \pm 1.15
	HGCN-PBMLR-P	89.05 \pm 0.78	85.04 \pm 0.97	75.89 \pm 0.78	77.90 \pm 1.00
	HGCN-BMLR-P	92.45 \pm 0.96	86.02 \pm 0.53	77.36 \pm 0.73	78.48 \pm 1.52
\mathbb{L}_K^n	HGCN	87.83 \pm 0.77	84.94 \pm 1.40	76.49 \pm 0.88	77.37 \pm 1.72
	HGCN-LMLR	89.72 \pm 1.51	82.61 \pm 1.01	75.44 \pm 1.17	69.91 \pm 3.61
	HGCN-BMLR-L	90.80 \pm 1.15	85.27 \pm 1.17	77.30 \pm 0.41	77.65 \pm 2.10

Table 7. Comparison of hyperbolic FC layers on link prediction. Best results within each hyperbolic model are in **bold**.

Graph for FC

Link prediction

Space	Method	Methodology	Disease $\delta = 0$	Airport $\delta = 1$	PubMed $\delta = 3.5$	Cora $\delta = 11$
\mathbb{P}_K^n	Möbius	Tangent	76.35 \pm 1.83	93.31 \pm 0.41	94.93 \pm 0.06	90.80 \pm 0.56
	Poincaré FC	Poincaré geometry	79.45 \pm 1.01	94.31 \pm 0.16	94.24 \pm 0.25	88.21 \pm 0.72
	BFC-P	Busemann	80.45 \pm 0.93	94.88 \pm 0.39	94.85 \pm 0.07	91.94 \pm 0.32
\mathbb{L}_K^n	LTFC	Tangent	71.32 \pm 5.36	92.68 \pm 0.35	94.85 \pm 0.17	89.37 \pm 0.64
	Lorentz FC	Ambient Minkowski	72.78 \pm 2.04	92.99 \pm 0.33	94.20 \pm 0.10	92.06 \pm 0.62
	BFC-L	Busemann	78.36 \pm 0.51	95.37 \pm 0.17	94.90 \pm 0.04	92.28 \pm 0.12

Thanks



Homepage



LinkedIn



UNIVERSITÀ
DI TRENTO



MAX PLANCK INSTITUTE
FOR INTELLIGENT SYSTEMS

